

\* Corresponding author: s.weiler@ihfg.uni-stuttgart.de; Homepage: <http://www.ihfg.uni-stuttgart.de>

# Phonon-Assisted Incoherent Excitation of a Quantum Dot and its Emission Properties

S. Weiler\*, A. Ulhaq, S. M. Ulrich, D. Richter, M. Jetter and P. Michler

*Institut für Halbleiteroptik und Funktionelle Grenzflächen,  
Universität Stuttgart, Allmandring 3, 70569 Stuttgart, Germany,*

C. Roy and S. Hughes

*Department of Physics, Engineering Physics and Astronomy,  
Queens's University, Kingston, Ontario, Canada K7L 3N6*

## Abstract

We present a detailed study of a phonon-assisted incoherent excitation mechanism of single quantum dots. A spectrally-detuned laser couples to a quantum dot transition by mediation of acoustic phonons, whereby excitation efficiencies up to 20 % with respect to strictly resonant excitation can be achieved at  $T = 9$  K. Laser frequency-dependent analysis of the quantum dot intensity distinctly maps the underlying acoustic phonon bath and shows good agreement with our polaron master equation theory. An analytical solution for the photoluminescence is introduced which predicts a broadband incoherent coupling process when electron-phonon scattering is in the strong phonon coupling (polaronic) regime. Additionally, we investigate the coherence properties of the emitted light and study the impact of the relevant pump and phonon bath parameters.

Important properties of non-classical light emission from a single quantum dot (QD), e.g. its exciton linewidth and coherence properties, depend on the physical nature of the excitation process of the QD. A standard method to optically address QDs is through excitation into the barrier or wetting layer, which causes subsequent capture and relaxation, finally resulting in the recombination of carriers and the emission of photons. Such an *incoherent pumping* mechanism leads to homogeneous broadening of the excited state and results in a reduction of coherence time. A more selective excitation of a single QD is possible via pumping into a higher electronic (d-, p-shell) or the QD ground state (s-shell). The latter technique is suitable to generate close to Fourier-transform-limited photons [1].

Due to distinct coupling of QD confined-state dynamics to the surrounding solid-state crystal, phonon-mediated excitation offers an alternative way of selective emitter state preparation. For instance, pumping of single QDs via the energetically sharp longitudinal-optical phonon (LO) resonance  $\sim 35$  meV above the dot ground state has been demonstrated [2–5]. Besides LO coupling, other optical excitation methods rely on the interaction of the electron-hole pair with acoustic phonons, for instance non-resonant coupling (NRC) between emitter and cavity [6–8]. This effect causes a detuned cavity mode to be efficiently excited by a QD coupled to the surrounding acoustic phonon bath. The inverse NRC effect, where the QD is excited via the cavity photon emission, has also been demonstrated experimentally [9]. Recent theoretical analysis in the context of the NRC effect, however, have shown that simple Lorentzian like pure-dephasing models are not sufficient to fully explain this phenomenon [6, 7, 10]. Especially in the domain of resonance fluorescence, where the QD-cavity system is excited coherently, significant phonon-induced coupling between the QD exciton and the cavity is predicted [11], resulting in phonon-mediated excitation-induced dephasing (EID) and pronounced exciton-cavity feeding. The former EID mechanism has been observed in micropillar-QD systems [12], and related EID phenomena have been measured using coherently excited QDs with pulsed lasers [13]; EID, via resonance fluorescence, manifests in spectral broadening of the Mollow triplet sidebands as the strength of the pump field is increased; however, it does not give any direct information about the spectral characteristics of the broad phonon bath. The exciton-acoustic phonon coupling is also directly observable via the broad phonon bands on the higher and lower energetic side of the zero-phonon line (ZPL) that can be theoretically explained by the independent boson

model [14] under consideration of pure dephasing effects [15]. The ZPL is Fourier-limited up to a first approximation but higher-order coupling terms lead to a broadening [16], which increases with temperature. These phonon-based pure dephasing effects have been experimentally studied in detail, particularly using the highly phase-sensitive technique of four-wave mixing [17]. The LA phonon sidebands have also been directly observed in QD emission spectra at elevated temperatures [18, 19], using incoherent excitation (i.e., pump laser excitation that is spectrally far detuned from the target exciton state).

In this Letter, we present a joint experimental-theory investigation of phonon-mediated incoherent excitation in the polaron regime. The clear signatures of phonon-mediated excitation is quite distinct to all previous attempts at exploring electron-phonon interactions in QDs, and we present an unequivocal and more direct probe of the phonon bath. We introduce an analytical model for the excited QD–phonon-bath system in a planar sample such that the coupling between laser photons and a QD is mediated by acoustic phonons in the framework of an effective phonon master equation (ME) [20], which is derived from a full polaron ME [11]. We show that the effective QD intensity is a direct result of phonon-mediated coupling which depends on the phonon density of states at the laser excitation energy and the pump intensity of the field. Moreover, this results in an incoherent excitation process that is a direct signature of exciton-phonon coupling effects beyond a weak exciton-phonon coupling approach—where such a mechanism is absent [21, 22]. Inspired by related theoretical predictions [20, 23], we experimentally demonstrate the effective pumping of a single QD via LA phonon coupling by spectrally tuning the laser close to the QD s-shell resonance within the range of LA phonon energies. The detuning-dependent frequency scans yield QD intensity profiles exhibiting both the ZPL profile along with the broad LA phonon sidebands (spanning more than 5 meV). Additionally we compare the coherence properties of the QD emission, excited via this incoherent excitation process driven by a coherent laser into the acoustic phonon bath with that of a resonantly excited QD.

For our experiments, we employed self-assembled In(Ga,As)/GaAs QDs grown by metal-organic vapor-phase epitaxy. A single layer of QDs was centered in a  $1\lambda$ -thick planar GaAs cavity surrounded by alternating  $\lambda/4$  periods of AlAs/GaAs as 4 top and 20 bottom distributed Bragg reflectors (DBR). The sample was mounted in a He-flow cryostat

at controllable temperatures of  $T = (4 - 15)$  K. For resonant laser stray-light suppression a orthogonal excitation-detection geometry micro photoluminescence ( $\mu$ PL) setup in combination with a pinhole assembly and polarizer was used. The sample was excited by a narrow band ( $\sim 500$  kHz) tunable Ti:Sapphire continuous wave laser. More details of the experimental techniques and the setup are given in Refs. [1, 24, 25].

Figure 1 illustrates the effect of phonon-assisted incoherent excitation of a QD. For the experimental conditions shown, the laser excitation is energetically blue-detuned from the emitter by  $\Delta = \hbar \cdot (\omega_L - \omega_{\text{QD}}) = 596 \mu\text{eV}$ . Even though the laser is not resonant with any higher QD shells (energetic separation between s- and p-shell separation is typically  $\sim 25$  meV), considerable emitter intensity can be observed in the  $\mu$ PL spectrum. The inset of Fig. 1 shows the corresponding auto-correlation measurement of QD photons unambiguously proving the single-photon emission nature with a  $g^{(2)}(0)$ -value of  $0.16 \pm 0.02$ , deconvoluted with respect to the setup time resolution of 450 ps (convoluted value:  $g^{(2)}(0) = 0.35 \pm 0.04$ ).

To gain more insight into the effect of the phonon-induced incoherent excitation, we scanned the cw laser over the QD resonance in steps of  $\sim 15 \mu\text{eV}$ . Under constant excitation power, a  $\mu$ PL spectrum is taken at each step ( $P = 500 \mu\text{W}$ ,  $T = 5$  K). The PL data depicted in Fig. 2 reveal appreciable QD emission over a long range of frequencies even away from the s-shell resonance. The persistent presence of the QD signal for a relatively large range of laser energies rules out excitation of the QD via the quantized energy eigenstates of the dot itself. Instead we attribute the excitation of the QD over a continuum of frequencies to the presence of the LA phonon bath. The QD is effectively excited by either emitting ( $\Delta > 0$ ) or absorbing ( $\Delta < 0$ ) phonons which compensate for the energy difference between the excitation source and the exciton s-shell energy. The inset of Fig. 2 (which shows a zoom into the region  $\Delta \approx 0$ ) displays the fine frequency scan over the QD s-shell with a step size of  $\sim 2 \mu\text{eV}$ . The increase of the signal towards  $\Delta = 0$  reflects the clear onset of resonance fluorescence (RF) which overtakes the laser stray-light intensity in the composite fluorescence and laser signal. Remarkably, such a pronounced phonon-coupling effect occurs even without any cavity coupling.

The effect of phonon-induced excitation is modeled using a polaronic ME where explicit

phonon-mediated processes have been considered and derived in the form of Liouvillian superoperators. A polaron ME has also been used to investigate QD Rabi oscillations [26]. The effective phonon model is explained in detail in Ref. [20], which also includes a cavity system. For the current system of interest (i.e., with no cavity coupling), the ME is [20]

$$\frac{\partial \rho}{\partial t} = \frac{1}{i\hbar} [H'_S, \rho(t)] + \frac{\gamma}{2} \mathcal{L}[\sigma^-] + \frac{\gamma'}{2} \mathcal{L}[\sigma_{11}] + \frac{\Gamma_{\text{ph}}^{\sigma^+}}{2} \mathcal{L}[\sigma^+] + \frac{\Gamma_{\text{ph}}^{\sigma^-}}{2} \mathcal{L}[\sigma^-], \quad (1)$$

with a polaron-transformed system Hamiltonian,  $H'_S = \hbar(-\Delta - \Delta_P)\sigma^+\sigma^- + \hbar\eta_x \langle B \rangle (\sigma^- + \sigma^+)$ , where  $\langle B \rangle = \exp\left[-\frac{1}{2} \int_0^\infty d\omega \frac{J(\omega)}{\omega^2} \coth(\beta\hbar\omega/2)\right]$  is the thermally-averaged bath displacement operator and  $J(\omega) = \alpha_p \omega^3 \exp(-\frac{\omega^2}{2\omega_b^2})$  is the characteristic phonon spectral function;  $\eta_x = 2\Omega$  is the coherent pump rate of the QD exciton,  $\sigma_{11} = \sigma^+\sigma^-$  with  $\sigma^+, \sigma^-$  the Pauli operators, and we will incorporate the polaron shift ( $\Delta_P$ ) into the definition of  $\omega_{QD}$  (and thus  $\Delta$ ) below. The Lindblad operators,  $\mathcal{L}[O] = 2O\rho O^\dagger - O^\dagger O\rho - \rho O^\dagger O$ , describe dissipation through ZPL radiative decay and ZPL pure dephasing ( $\gamma'$ ), as well as pump-driven incoherent scattering processes mediated by the phonon bath:  $\Gamma_{\text{ph}}^{\sigma^+/\sigma^-} = 2\langle B \rangle^2 \eta_x^2 \text{Re} \left[ \int_0^\infty d\tau e^{\pm i\Delta\tau} (e^{\phi(\tau)} - 1) \right]$ , where  $\phi(\tau) = \int_0^\infty d\omega \frac{J(\omega)}{\omega^2} [\coth(\hbar\omega/2k_bT) \cos(\omega\tau) - i \sin(\omega\tau)]$ . Physically, the  $\Gamma_{\text{ph}}^{\sigma^-}$  process corresponds to an enhanced radiative decay, while the  $\Gamma_{\text{ph}}^{\sigma^+}$  process represents an incoherent excitation process. If the laser pump is within the vicinity of the phonon bath, then the QD exciton can be excited through phonon emission or absorption [20]. As well as having analytical phonon scattering rates in the polaronic regime, we can also use Eq. (1) to derive an explicit expression for the steady-state exciton population (see Supplementary Material),

$$\bar{N}_x = \frac{1}{2} \left[ 1 + \frac{\Gamma_{\text{ph}}^{\sigma^+} - \Gamma_{\text{ph}}^{\sigma^-} - \gamma}{\Gamma_{\text{ph}}^{\sigma^+} + \Gamma_{\text{ph}}^{\sigma^-} + \gamma + \frac{4\eta_x^2 \langle B \rangle^2 \Gamma_{\text{pol}}}{\Gamma_{\text{pol}}^2 + \Delta^2}} \right], \quad (2)$$

where  $\Gamma_{\text{pol}} = \frac{1}{2}(\Gamma_{\text{ph}}^{\sigma^+} + \Gamma_{\text{ph}}^{\sigma^-} + \gamma + \gamma')$ . For the planar system of interest, the QD intensity from the vertical decay channel of the sample is simply  $I_{QD} \propto \bar{N}_x$ . Importantly, Eq. (2) includes the detuning and pump dependence of the phonon-induced scattering rates. We stress again that the incoherent excitation process described through  $\mathcal{L}[\sigma^+]$  [see inset to Fig. (4) for a schematic picture of this process] does not appear in ME approaches that assume weak exciton-phonon coupling. Thus, our PL lineshapes (measured and predicted) show clear evidence of polaronic behaviour via phonon-bath-mediated incoherent excitation.

To compare with the theoretical predictions of Eq. (2), the experimentally derived near-resonance  $\mu\text{PL}$  scans have been evaluated in terms of normalized QD intensity versus detuning. The results of a scan as shown in Fig. 2 are displayed in Figs. 3(a) and 3(b) [black data

points] revealing strong resonance fluorescence of the QD near  $\Delta \approx 0$  and a less intense, but distinctly broad QD emission with a corresponding detuning range between  $\Delta \approx -1.5$  meV and  $+2$  meV. The above presented theoretical model has been fitted to the experimental data [red solid lines in Figs. 3(a) and 3(b)]. The depicted profiles consists of two parts, i.e., a rather *sharp* ZPL (Lorentzian profile) at the QD resonance and a broader phonon-assisted excitation feature around the ZPL. In the latter case, a distinct asymmetry for  $\Delta > 0$  is clearly visible. This is a direct and unambiguous signature of the unequal probabilities for LA phonon absorption and emission at low temperatures. This incoherent scattering process is quite different to the incoherent feeding that would result from a fast inter-level decay process. To help identify this process further, we also plot the calculation when the  $\Gamma_{\text{ph}}^{\sigma^+}$  process is turned off, which confirms that the laser-driven incoherent excitation process is the dominant phonon scattering process.

For modeling the measurement data, the corresponding values for temperature  $T$ , pump rate  $\eta_x$ , and radiative decay  $\gamma$ , have been experimentally derived by independent measurements and are therefore fairly accurate values within their experimental error. As is shown in the inset graph,  $\eta_x$  can be extracted from the HRPL data. For the conditions in Fig. 3(a) the center to sideband Rabi-splitting  $\Omega$  is found to be  $(16.7 \pm 0.7) \mu\text{eV}$  ( $= 4.04 \pm 0.17$  GHz), giving  $\eta_x = \frac{2\Omega}{2\pi} = (5.32 \pm 0.23) \mu\text{eV}$ . The radiative lifetime for most of the QDs in the sample is found to be rather similar due to no preferential radiative enhancement of selective QDs by Purcell-like effects. Independent time-correlated photon counting measurements have revealed a typical radiative decay time of (750 - 850) ps which gives  $\gamma \approx (0.77 - 0.88) \mu\text{eV}$ . The coupling constant describing the interaction between the exciton and the LA phonons via deformation potential  $\alpha_p$ , the pure dephasing rate  $\gamma'$  and the cut-off frequency  $\omega_b$  (proportional to the inverse of the typical electronic localization length in the QD) [21] are then derived via fitting. It should be mentioned that in most of our measurements we observed somewhat higher QD intensities than theoretically expected for intermediate positive detunings (as visible in Fig. 3(a) around  $\Delta = 2$  meV and 3(b) around  $\Delta = 1.7$  meV). This effect might be attributed to some additional dephasing apart from the LA phonon coupling which could be caused by a variety of possible effects like phonon scattering from defects or trapped charges in the vicinity of the QD [19]. Excitation via phonon-coupling is observed to be rather efficient and approximately 20 % of the QD intensity is achieved with respect to strictly resonant excitation with the distinct advantage that the laser stray-light

can be easily separated from the QD emission; this efficient phonon-induced excitation is unique to the QD environment and is substantially different to exciting an atomic resonance.

Photon-visibility measurements have been performed by Michelson interferometry to determine the coherence properties of photons emitted by both resonant and off-resonant excitation conditions. Figure 3(c) shows the sinusoidally-varying visibility of the QD emission under strictly resonant excitation which indicates the presence of the Mollow triplet [27, 28] in the spectral regime. The data has been fitted by the following function  $g^{(1)}(\tau) = \frac{1}{2}e^{-\Gamma_{\text{pol}}\tau}e^{i\omega\tau} + \frac{1}{4}e^{-(\Gamma_{\text{tot}}/2)\tau}e^{i(\omega-\Omega)\tau} + \frac{1}{4}e^{-(\Gamma_{\text{tot}}/2)\tau}e^{i(\omega+\Omega)\tau}$ , with  $\Gamma_{\text{tot}} = \Gamma_{\text{pol}} + \Gamma_{\text{pop}}$  and  $\Gamma_{\text{pop}} = \gamma + \Gamma_{\text{ph}}^{\sigma^+} + \Gamma_{\text{ph}}^{\sigma^-}$ , where the exponential decay reflects the limited coherence yielding a  $T_2 = (258 \pm 31)$  ps. Even under strictly resonant excitation the coherence is not lifetime limited, which may be attributed to spectral diffusion effects. As a comparison, we experimentally investigated the emission coherence under the non-resonant excitation conditions of phonon-assisted excitation for different detunings  $\Delta$ . The Gaussian fitting functions applied to the measurement results shown in Fig. 3(d-f) reveal coherence times of  $T_2 \sim 20$  ps rather limited compared to the value under resonant pump due to dephasing induced by the excitation mechanism.

To gain further insight into the effect of phonon-assisted incoherent excitation, we have systematically studied theoretically the effects of  $\omega_b$ ,  $T$ ,  $\alpha_p$ ,  $\eta_x$  on the resulting intensity profiles in Figs. 4 (a-d). An increase in the cut-off frequency  $\omega_b$  (i.e., a decrease in QD size) leads to a blue shift of the phonon reservoir replica of the QD intensity profile. In contrast, increasing temperature  $T$ , pump rate  $\eta_x$  or coupling factor  $\alpha_p$  overall increases the QD intensity for off-resonant excitation conditions. This can also be seen in Figs. 3 (a) and (b), where increased temperature and pump rate leads to a higher emission efficiency in 3(b) as compared to 3(a). For increasing temperature, these features become more symmetric due to increasing phonon state occupations. Parameters  $\alpha_p$  and  $\eta_x$  have similar effects on the shape of the intensity profile but keep the asymmetry unchanged. Variation of  $\gamma, \gamma'$  (not shown) mainly affects the width of the ZPL and has almost negligible effect on the broader intensity profile. We would like to emphasize that the effect has been observed consistently for several QDs in the sample. The investigations are also particularly important for experiments under pulsed resonant excitation. Here the spectrally broad laser (compared

to cw excitation) has distinct overlap not only with the ZPL, but also with the acoustic phonon side wings. Therefore the resonance fluorescence signal has additional contributions from photons emitted after phonon-induced coupling, which might increase the excitation efficiency but also change the coherence properties of the detected photons.

In conclusion, we have presented a detailed study of the phonon-assisted incoherent excitation effect for self-assembled QDs. The experimentally investigated dot intensity as a function of laser-QD detuning is in very good agreement with a polaronic ME model. Additionally, we have studied the coherence properties of QD emission via the phonon-mediated excitation and the influence of different realistic parameters on the spectral shape of the intensity profile has been theoretically investigated, using a newly presented analytical solution for the steady-state exciton population. Phonon-assisted incoherent excitation therefore does not only provide a unique excitation mechanism of a semiconductor QD but also an effective new tool to map the characteristic features of the phonon bath present in such a solid state quantum-emitter system. This process is also polaronic in nature, demonstrating exciton-phonon coupling effects beyond the weak coupling regime.

We thank W.-M. Schulz for expert sample preparation. S. Weiler acknowledges financial support by the Carl-Zeiss-Stiftung. A. Ulhaq acknowledges funding from International Max Planck Research School IMPRS-AM. This work was supported by the National Sciences and Engineering Research Council of Canada.

- 
- [1] S. Ates, S. M. Ulrich, S. Reitzenstein, A. Löffler, A. Forchel, and P. Michler, *Phys. Rev. Lett.* **103**, 167402 (2009).
  - [2] A. Lemaître, A. D. Ashmore, J. J. Finley, D. J. Mowbray, M. S. Skolnick, M. Hopkinson, and T. F. Krauss, *Phys. Rev. B* **63**, 161309(R) (2001).
  - [3] Y. Toda, O. Moriwaki, M. Nishioka, and Y. Arakawa, *Phys. Rev. Lett.* **82**, 4114 (1999).
  - [4] F. Findeis, A. Zrenner, G. Böhm, and G. Abstreiter, *Phys. Rev. B* **61**, 10579(R) (2000).
  - [5] R. Oulton, J. J. Finley, A. I. Tartakovskii, D. J. Mowbray, M. S. Skolnick, M. Hopkinson, A. Vasanelli, R. Ferreira, and G. Bastard, *Phys. Rev. B* **68**, 235301 (2003).



- [6] S. Hughes, P. Yao, F. Milde, A. Knorr, D. Dalacu, K. Mnaymneh, V. Sazonova, P. J. Poole, G. C. Aers, J. Lapointe, R. Cheriton, and R. L. Williams, *Phys. Rev. B* **83**, 165313 (2011).
- [7] M. Calic, P. Gallo, M. Felici, K. A. Atlasov, B. Dwir, A. Rudra, G. Biasiol, L. Sorba, G. Tarel, V. Savona, and E. Kapon, *Phys. Rev. Lett.* **106**, 227402 (2011).
- [8] A. Majumdar, E. D. Kim, Y. Gong, M. Bajcsy, and J. Vučković, *Phys. Rev. B* **84**, 085309 (2011).
- [9] M. Kaniber, A. Neumann, A. Laucht, M. F. Huck, M. Bichler, M.-C. Amann and J. J. Finley, *New Journal of Physics* **11**, 013031 (2009).
- [10] U. Hohenester, *Phys. Rev. B*, **81**, 155303 (2010).
- [11] C. Roy and S. Hughes, *Phys. Rev. Lett.* **106**, 247403 (2011).
- [12] S. M. Ulrich, S. Ates, S. Reitzenstein, A. Löffler, A. Forchel and P. Michler, *Phys. Rev. Lett.* **106**, 247402 (2011).
- [13] A. J. Ramsay, Achanta Venu Gopal, E. M. Gauger, A. Nazir, B. W. Lovett, A. M. Fox, and M. S. Skolnick, *Phys. Rev. Lett.* **104**, 017402 (2010).
- [14] G. D. Mahan *Many particle physics*, (Springer, Berlin Heidelberg, 2000)
- [15] T. Takagahara, *Phys. Rev. B* **60**, 2638 (1999).
- [16] E. A. Muljarov, and R. Zimmermann, *Phys. Rev. Lett.* **93**, 237401 (2004).
- [17] P. Borri, W. Langbein, U. Woggon, V. Stavarache, D. Reuter and A. D. Wieck, *Phys. Rev. B* **71**, 115328 (2005).
- [18] L. Besombes, K. Kheng, L. Marsal, and H. Mariette, *Phys. Rev. B* **63**, 155307 (2001).
- [19] I. Favero, G. Cassabois, R. Ferreira, D. Darson, C. Voisin, J. Tignon, C. Delalande, G. Bastard, Ph. Roussignol, and J. M. Gérard, *Phys. Rev. B* **68**, 233301 (2003).
- [20] C. Roy and S. Hughes, *Phys. Rev. X* **1**, 021009 (2011).
- [21] A. Nazir, *Phys. Rev. B* **78**, 153309 (2008).
- [22] A. Moelbjerg, P. Kaer, M. Lorke, and J. Mørk, *Phys. Rev. Lett.* **108**, 017401 (2012)
- [23] K. J. Ahn, J. Förstner, and A. Knorr, *Phys. Rev. B* **71**, 153309 (2005).
- [24] S. Ates, S. M. Ulrich, A. Ulhaq, S. Reitzenstein, A. Löffler, S. Höfling, A. Forchel, and P. Michler, *Nature Phot.* **3**, 724 (2009).
- [25] A. Ulhaq, S. Ates, S. Weiler, S. M. Ulrich, S. Reitzenstein, A. Löffler, S. Höfling, L. Worschech, A. Forchel, and P. Michler, *Phys. Rev. B* **82**, 045307 (2010).
- [26] D. P. S. McCutcheon and A. Nazir, *New J. Phys.* **12**, 113042 (2010).

- [27] B. R. Mollow, *Phys. Rev.*, 188 (1969).
- [28] A. Muller, E. B. Flagg, P. Bianucci, X. Y. Wang, D. G. Deppe, W. Ma, J. Zhang, G. J. Salamo, M. Xiao, and C. K. Shih, *Phys. Rev. Lett.* **99**, 187402 (2007).

Figures

Figure 1, S. Weiler, P.R.L.

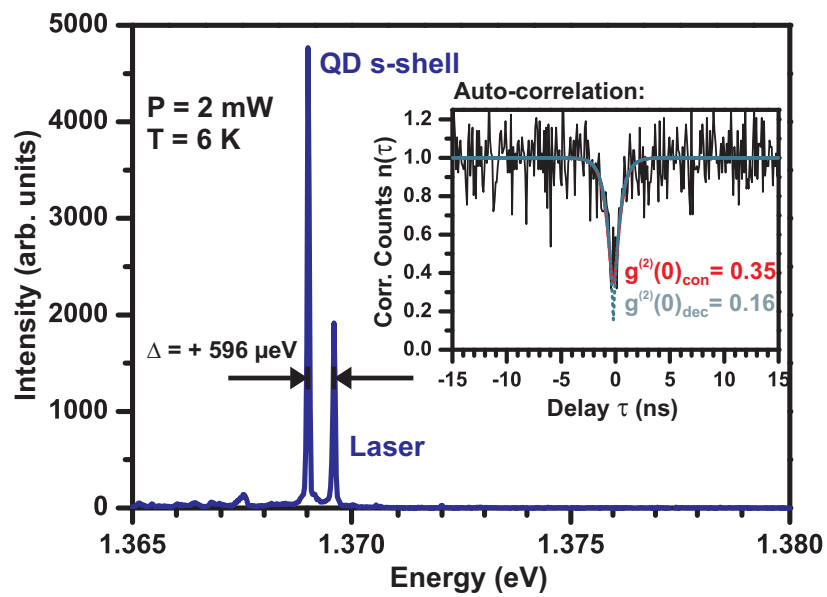


Figure 2, S. Weiler, P.R.L.

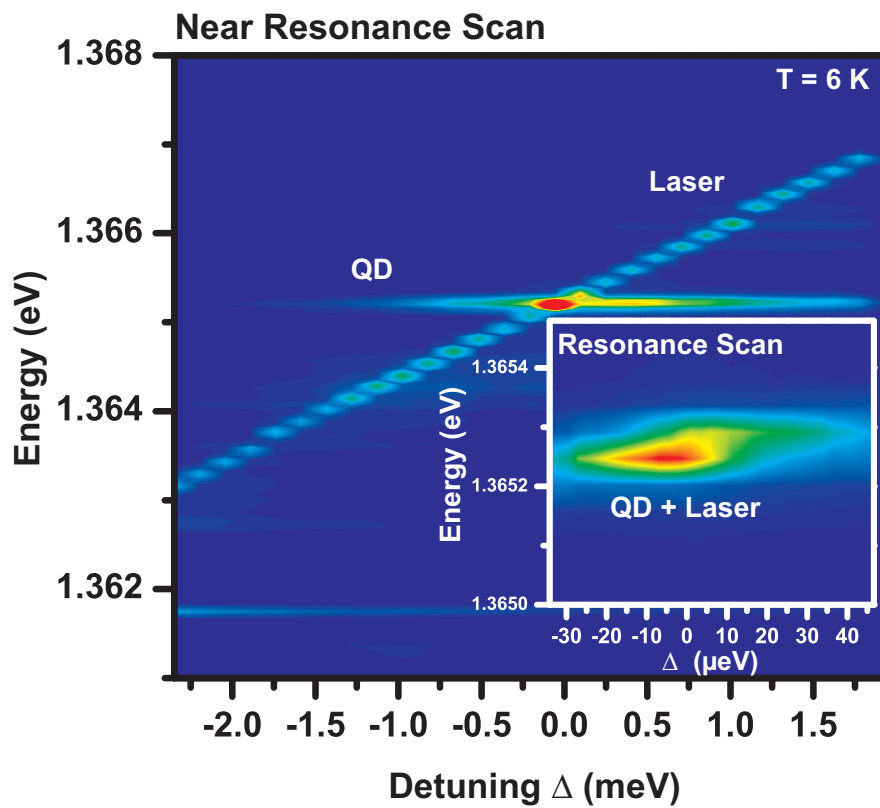


Figure 3, S. Weiler, P.R.L.

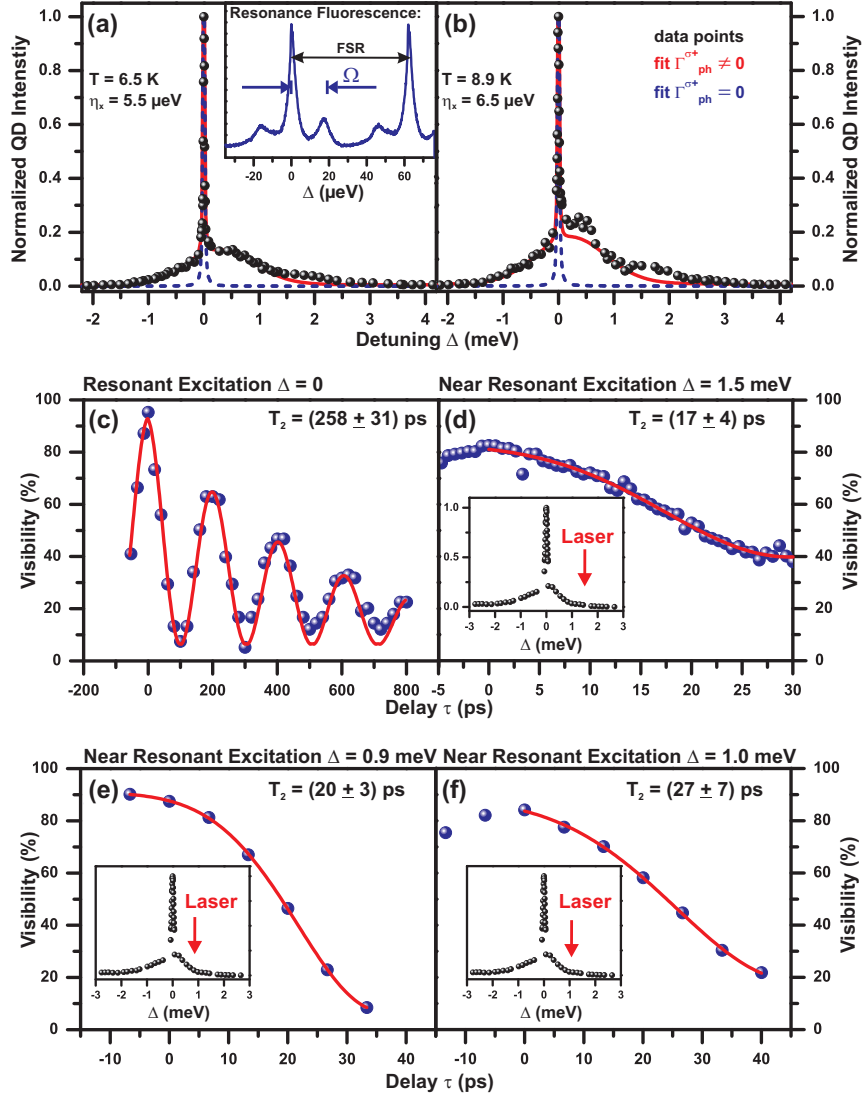
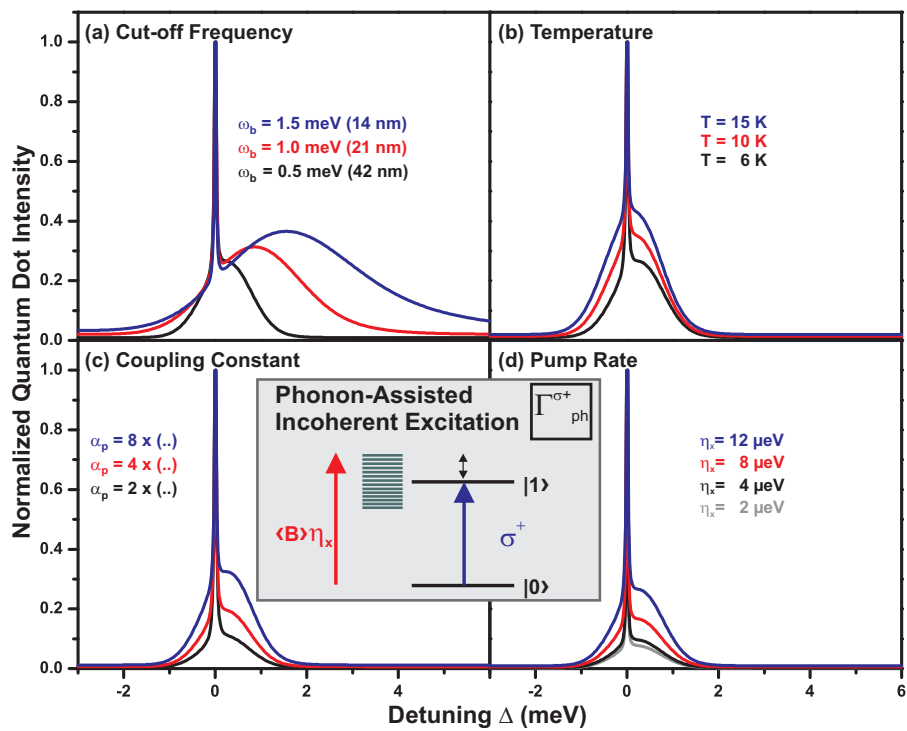


Figure 4, S. Weiler, P.R.L.



## Figure Captions

**FIG.1** Demonstration of phonon-assisted incoherent excitation of a single QD. PL emission spectrum of a QD non-resonantly excited via a cw laser ( $\Delta = 596$  meV) Inset: Corresponding auto-correlation measurement on the QD s-shell proving almost background-free single-photon emission with a deconvoluted antibunching value (detector response) of  $g^{(2)}(0)_{\text{dec}} = 0.16 \pm 0.02$  (convoluted:  $g^{(2)}(0)_{\text{con}} = 0.35 \pm 0.04$ ).

**FIG.2** Near resonance frequency scan: The excitation laser energy has been systematically varied in steps of  $\sim 15$   $\mu\text{eV}$  to scan over the QD s-shell at a fixed power of  $P = 500$   $\mu\text{W}$ . As evident from the color plot, emission from the QD can be continuously traced. Inset: Resonance scan: Detailed scan over the QD s-shell in steps of  $\sim 2$   $\mu\text{eV}$  revealing the onset of RF around  $\Delta = 0$ .

**FIG.3** (a)-(b) Intensity profiles: Integrated QD intensity derived from a frequency scan (similar to that in Fig. 2) plotted as a function of laser-QD detuning. The scans have been performed at different temperatures. Experimental data indicated by black circles and theory (red solid lines). The corresponding values used to fit the data with our theory (with phonon-induced processes  $\Gamma_{\text{ph}}^{\sigma^+}$  and  $\Gamma_{\text{ph}}^{\sigma^-}$ : solid (red) line, with only the process  $\Gamma_{\text{ph}}^{\sigma^-}$ : dashed (blue) line) are the cut-off frequency  $\omega_b = 0.6$  meV, coupling parameter  $\alpha_p = 6 \times 0.06 \times \pi^2$  ps, rate of radiative decay rate  $\gamma = 0.82$   $\mu\text{eV}$  (803 ps) and pure dephasing rate  $\gamma' = 0.6$   $\mu\text{eV}$  (1097 ps). The thermally-averaged bath displacement operator is calculated to be  $\langle B \rangle = 0.91$  for the conditions in (a) and  $\langle B \rangle = 0.87$  for (b). Inset: HRPL spectrum with the characteristic RF spectrum in the frequency domain, revealing a Rabi energy (center to sideband) of  $\Omega = (16.7 \pm 0.7)$   $\mu\text{eV}$ . (c) Visibility measurements under strictly resonant and off-resonant (d-f) phonon-assisted incoherent excitation conditions. The off-resonant emission reveals a distinctly shorter  $T_2$  of  $(17 \pm 4)$  ps for  $\Delta = 1.5$  meV,  $(20 \pm 3)$  ps for  $\Delta = 0.9$  meV and  $(27 \pm 7)$  ps for  $\Delta = 1.0$  meV, in comparison to the resonant coherence of  $(258 \pm 31)$  ps attributed to the phonon emission dephasing process. The solid lines are the corresponding gaussian fits to the experimental data.

**FIG.4** Investigation of the influence of the relevant parameters on the intensity profile of the QD emission. While keeping the other parameters fixed ( $\omega_b = 0.5$  meV,  $T = 6$  K,  $\gamma = 0.8$   $\mu$ eV (823 ps),  $\gamma' = 0.8$   $\mu$ eV,  $\eta_x = 12$   $\mu$ eV), the (a) phonon bath cut-off frequency  $\omega_b$ , (b) temperature  $T$ , (c) coupling factor  $\alpha_p$ , and (d) pump rate  $\eta_x = 2\Omega$  have been systematically increased from bottom to top respectively. Inset: Illustration of the incoherent excitation process (red arrow),  $\Gamma_{\text{ph}}^{\sigma^+}$  scattering, mediated by the acoustic phonon bath (green lines).